How Resource Phenology Affects Consumer Population Dynamics

Sharon Bewick,[1],* R. Stephen Cantrell,[2] Chris Cosner,[2] and William F. Fagan[1]

[1]Department of Biology, University of Maryland, College Park, Maryland 20742;   [2]Department of Mathematics, University of Miami, Miami, Florida 33124

ABSTRACT: Climate change drives uneven phenology shifts across taxa, and this can result in changes to the phenological match between interacting species. Shifts in the relative phenology of partner species are well documented, but few studies have addressed the effects of such changes on population dynamics. To explore this, we develop a phenologically explicit model describing consumer-resource interactions. Focusing on scenarios for univoltine insects, we show how changes in resource phenology can be reinterpreted as transformations in the year-to-year recursion relationships defining consumer population dynamics. This perspective provides a straightforward path for interpreting the long-term population consequences of phenology change. Specifically, by relating the outcome of phenological shifts to species traits governing recursion relationships (e.g., consumer fecundity or competitive scenario), we demonstrate how changes in relative phenology can force systems into different dynamical regimes, with major implications for resource management, conservation, and other areas of applied dynamics.

Keywords: phenology mismatch, consumer-resource dynamics, recursion relationship, nonautonomous ordinary differential equation, Zonneveld equation, chaos.

Global change processes are leading to substantial shifts in species phenology (Parmesan 2007; Sherry et al. 2007; Zhang et al. 2007; Thackeray et al. 2010). In general, most species have exhibited earlier phenology with increased global temperatures (Root et al. 2003). However, across species, temperature effects vary widely (Bale et al. 2002). This can be a result of different reaction norms, development thresholds, or degree-day requirements (Watt and McFarlane 2002). Alternately, it can depend on differences in habitat use or behavior (Singer and Parmesan 2010) that lead to species experiencing different ambient conditions in the field (Bale et al. 2002). Species can also differ in their use of temperature cues for timing critical life events (Kudo et al. 2004). Different species may, for instance, synchronize their life cycles on the basis of temperatures at different times in the year (Doi et al. 2008) or at different locations in space (e.g., during migration; Jones and Cresswell 2010). Alternately, species may have different temperature requirements (e.g., winter chilling/vernalization) that have contrasting effects on phenology (Zhang et al. 2007; Forrest and Miller-Rushing 2010). Finally, species may vary in the extent to which they use temperature cues at all (Tauber and Tauber 1976).

Interspecific variation in phenological shifts is particularly worrisome when different functional groups and trophic levels respond in different ways (Parmesan 2007; Thackeray et al. 2010). Such variation increases the likelihood of phenological mismatch among interacting species (Durant et al. 2007; Memmott et al. 2007; Both et al. 2009; Singer and Parmesan 2010). This can be devastating if one or both species rely on the other for survival (Miller-Rushing et al. 2010). A common example is consumer-resource interactions (Cushing 1990; Durant et al. 2007; Kerby et al. 2012; Revilla et al. 2014). Often, there is a tight requirement on consumers to emerge at the same time as their resource. If they emerge too early, the resource will not be present, and the consumer will risk starvation. If they emerge too late, the resource may have senesced or may be of poorer quality. Again, consumer survival will be compromised (Harrington et al. 1999; Visser and Both 2005; van Asch and Visser 2007).

Intuitively, one might expect that there would be strong selection on processes governing phenological synchrony among pairs of closely interacting species (van Asch and Visser 2007). Although this is likely true within the context of conditions that have occurred over evolutionary history, climate change may result in novel regimes not experienced during the course of evolution. Thus, mechanisms that have evolved to yield synchrony among interacting species may break down (Visser and Both 2005; Miller-Rushing et al. 2010).

Plant-insect interactions are a clear example where changing phenology between a host plant and its herbivores can have dramatic consequences on herbivore abundance (McLaughlin et al. 2002). However, while there has been clear demonstration that phenology can affect insect herbivore

populations, it is less clear exactly how this depends on the nature of the phenological change and the life-history traits of the plant and insect species involved. In this article, we consider a phenologically explicit model of the interaction between a host plant and an obligate univoltine insect consumer. We focus on a specialist species, because specialists are predicted to suffer most from phenological mismatch (van Asch and Visser 2007; Miller-Rushing et al. 2010; Donnelly et al. 2011). Using our model, we show how resource phenology interacts with the consumer population to determine population-level properties, including survival and dynamics. Although our model assumes particular forms of interaction between the consumer and its resource, more broadly our goal is to illustrate a general approach for interpreting the long-term consequences of phenological mismatch. Specifically, we show how species recursion relationships can be leveraged as a conceptual tool for predicting the outcome of phenology change and population dynamics, providing a modeling framework within which additional complications, such as differing life histories, differing physiologies, and mechanistic responses to climatic cues could ultimately be considered.

Method

Dynamics

Because we are interested in the long-term consequences of phenology, two timescales are important: within-season dynamics and multiyear dynamics. Within-season dynamics determine the success or failure of the population over the course of a single year. For univoltine consumer species, within-season dynamics account for processes such as emergence, competition, and death. In contrast, multiyear dynamics map the net success of a population from one year to the next. Multiyear dynamics account for birth and overwintering, wherein adults that remain at the end of one growing season leave offspring that emerge at the start of the next. In general, phenology change will exert its effect on a within-season timescale. However, because phenological changes can affect interacting populations through their demographics (Miller-Rushing et al. 2010), shifts in phenology will also have consequences on multiyear timescales. Understanding the connection between these two timescales enables prediction of the long-term consequences of phenology change.

Within-Season Dynamics. We develop a nonautonomous differential-equation system for within-season dynamics. This approach builds on similar models that have been used to study reproductive asynchrony within single populations (Zonneveld and Metz 1991; Zonneveld 1992) and in two-sex populations (Calabrese et al. 2008; Fagan et al. 2010; Larsen et al. 2013; Lynch et al. 2014). For a season that runs

from time $t = 0$ to time $t = t_\mathrm{f}$ (where t_f denotes the maximum life span or maturation period of the consumer), we assume the following within-season dynamics:

$$\frac{dC}{dt} = \overbrace{\hat{C}g_\mathrm{c}(t, \theta_\mathrm{c})}^{\text{emergence}} - \overbrace{h(C, R)}^{\text{starvation}} - \overbrace{\alpha_\mathrm{c}C}^{\substack{\text{constant}\\\text{mortality}}}, \quad (1a)$$

$$\frac{dR}{dt} = \overbrace{\hat{R}g_\mathrm{r}(t, \theta_\mathrm{r})}^{\text{emergence}} - \overbrace{m(C, R)}^{\substack{\text{loss due to}\\\text{consumer action}}} - \overbrace{\alpha_\mathrm{r}R}^{\substack{\text{constant}\\\text{mortality}}}. \quad (1b)$$

In equations (1), C and R are the consumer and resource populations at time t, respectively. In equation (1a), $\hat{C}$ is the total, season-long consumer population, $g_\mathrm{c}(t, \theta_\mathrm{c})$ is a probability density function that captures consumer phenology by defining consumer emergence as function of time ($\int_0^{t_\mathrm{f}} g_\mathrm{c}dt = 1$), α_c is the density-independent death rate of the consumer, and $h(C, R)$ is a general function describing the death rate of the consumer as a result of starvation. Likewise, in equation (1b), $\hat{R}$ is the total, season-long resource population, $g_\mathrm{r}(t, \theta_\mathrm{r})$ is a probability density function that captures resource phenology by defining resource emergence as function of time ($\int_0^{t_\mathrm{f}} g_\mathrm{r}dt = 1$), α_r is the natural death rate of the resource, and $m(C, R)$ is a general function describing losses to the resource population due to actions of the consumer. Here, θ_c and θ_r are vectors of parameters defining the shapes of the consumer and resource emergence functions, respectively (see eqq. [3]).

Importantly, because we are modeling a univoltine insect, there is no resource-dependent birth term in the within-season consumer equation (1a). This is in contrast to more common consumer-resource models (e.g., Lotka-Volterra, MacArthur-Rosenzweig), where the effect of the resource is to modulate consumer birth rate. In our model, the resource instead mediates larval starvation, which is in keeping with the ecology of several different insect defoliators, for example, checkerspot butterflies *Euphydryas editha* (White 1974), Colorado potato beetles *Leptinotarsa decemlineata* (Morris 1997), and goldenrod leaf beetles *Trirhabda* spp. (Brown and Weis 1995). Our model could also accommodate resource effects on consumer fecundity. However, this would have to appear in our equations for multiyear dynamics (see eqq. [2]), rather than as a continuous birth term. Note also that, because of its general form, $m(C, R)$ in the resource equation (1b) can represent losses that extend far beyond host consumption to include any effects that make host plants unavailable to the consumer population, including defoliation that outpaces regrowth, induced defenses, girdling of branches, or resource mortality.

Multiyear Dynamics. To map population success at the end of season N to total population emergence in season $N + 1$, we apply the following multiyear dynamics:

$$\hat{C}_{N+1} = \sigma C_N(t_f) \equiv f(\hat{C}_N), \tag{2a}$$

$$\hat{R}_{N+1} = \hat{R}_N \equiv \text{constant}, \tag{2b}$$

where σ is a combined parameter accounting for consumer fecundity and consumer death due to overwintering (i.e., net fecundity), $C_N(t_f)$ is consumer density at the end of season N, and $\hat{C}_N$ and $\hat{R}_N$ are, as above, the total season-long consumer and resource populations, respectively, in year N. In equations (2), we have assumed that end-of-season consumer density in year N determines the total population of consumers that will emerge in year $N + 1$; thus, the year-to-year map describing the total season-long consumer population is a complex function, $f(\hat{C}_N)$, that depends on within-season dynamics $C_N(t)$ and fecundity/overwintering success σ. In contrast, we have assumed that the total population of resource that will emerge in year $N + 1$ is independent of the standing resource density at the end of season N (Crawley 1989; Murdoch et al. 2002); thus, the total resource population that emerges over the course of a season is the same from one year to the next. This simplistic assumption for resource dynamics allows us to focus on the more complicated dynamics of the consumer population. It is a good approximation for resources with an annual lifestyle and recruitment constrained by limiting factors (e.g., space, nutrients) other than seed production. It is also a good approximation for long-lived resources with a perennial lifestyle, provided that aboveground biomass at the end of one season is only weakly coupled to aboveground biomass production the following year. An alternative model with feedback from one season to the next would be required for a resource that exhibits seed limitation or strong correlations in year-to-year aboveground biomass.

Emergence and Loss Functions

To explore the behavior of our consumer-resource model, we must first specify emergence (g_c, g_r) and loss (h, m) functions. While our general approach could be applied to any choice of g_c, g_r, h, and m, we demonstrate our method by assuming functions that are sufficiently broad to encompass a range of different dynamic behaviors but at the same time specific enough to represent the life histories of particular plant herbivores (e.g., Lepidoptera). For emergence, we assume gamma distributions; the advantages of gamma distributions in the context of phenologically explicit models are discussed at length elsewhere (Calabrese et al. 2008). Specifically, we use

$$g_c(t, \theta_c) = \begin{cases} 0 & t < \varepsilon_c, \\ \dfrac{\lambda_c}{\Gamma(\phi_c)} [\lambda_c(t - \varepsilon_c)]^{\phi_c - 1} e^{-\lambda_c(t - \varepsilon_c)} & t > \varepsilon_c, \end{cases} \tag{3a}$$

$$g_r(t, \theta_r) = \begin{cases} 0 & t < \varepsilon_r, \\ \dfrac{\lambda_r}{\Gamma(\phi_r)} [\lambda_r(t - \varepsilon_r)]^{\phi_r - 1} e^{-\lambda_r(t - \varepsilon_r)} & t > \varepsilon_r, \end{cases} \tag{3b}$$

where Γ is the gamma function and $\theta_\varsigma = (\lambda_c, \phi_c, \varepsilon_c)$, with $\varsigma = c, r$, are parameter vectors whose elements describe the scale (λ_c) and shape (ϕ_c) parameters of the gamma distribution and the shift parameter (ε_c) that varies as a function of phenology.

Loss functions are more complicated. First, few consumer-resource models consider consumer starvation, which can be important in the context of phenology mismatch. Second, most consumer-resource models assume mass-action kinetics, potentially subject to consumer satiation. However, in plant-insect systems, consumers are often physically located on their resource. Thus, rather than the "contact rate" paradigm that predominates in Lotka-Volterra, MacArthur-Rosenzweig, and other classical consumer-resource models, consumer survival in our systems is instead determined by whether or not host plants can support a particular level of infestation (White 1974; Brown and Weis 1995; Morris 1997; Broberg et al. 2002). One way to capture this is to assume that consumer survival depends on the average consumer load per plant (C/R). Consequently, we suggest the following "Hill" function for consumer starvation:

$$h(C, R) = \frac{d_c [C/(R + \delta)]^x C}{K_c + [C/(R + \delta)]^x} \approx \frac{d_c (C/R)^x C}{K_c + (C/R)^x}. \tag{4a}$$

In equation (4a), d_c is the maximum death rate of consumers, K_c is the half-maximum number of consumers that a host plant can support, x determines the steepness of starvation onset as a function of consumer load per plant, and $\delta \ll 1$ is a small number used to ensure that h remains finite as $R \to 0$.

There are two advantages of the Hill function formulation. First, Hill functions are flexible. This allows for a wide variety of different functional responses, ranging from a saturating response to responses with strong thresholds, depending on the choice of Hill parameters. Second, when a Hill function is used to describe consumer losses, the Hill exponent, x, can be naturally interpreted as a measure of consumer dispersion. This allows us to consider system behavior as a function of the degree of consumer aggregation. When x is small, consumers are highly aggregated. As a result, some fraction of host plants are heavily infested, even at low consumer densities ($C/R < K_c$); however, by the same token, some fraction of host plants have low consumer abundance, even at high consumer densities ($C/R > K_c$). As a result, consumer starvation increases gradually with increasing consumer density. In contrast, when x is large, consumers are overdispersed/distributed evenly across plants. Consequently, most host plants have equivalent numbers of con-

sumers, and the transition to an unsustainable consumer population occurs synchronously across all plants at $C/R = K_c$. In the limit that $x \to \infty$, the Hill function becomes a step function, which corresponds to a perfectly uniform distribution of consumers over host plants.

Depending on the system, heavy levels of consumer infestation may exacerbate consumer starvation by actively damaging host plants (e.g., girdling or defoliating existing growth faster than host plants can regenerate new growth). To capture this effect, we use another Hill function, specifically,

$$m(C, R) = \frac{d_r[C/(R + \delta)]^x R}{K_r + [C/(R + \delta)]^x} \approx \frac{d_r(C/R)^x R}{K_r + (C/R)^x}. \quad (4b)$$

In equation (4b), we allow resource damage to occur at a different rate (d_r) and at a different infestation threshold (K_r), as compared to consumer starvation. In contrast, we assume that the steepness, x, is identical for the consumer and resource responses (loosely representing the level of consumer dispersion).

For the analysis presented in the main text, we focus on two scenarios that serve to illustrate the two extremes of model behavior. First, we consider a system with concomitant consumer starvation and resource degradation: $d_c = d_r \equiv d$, $K_r = K_c \equiv K$. This represents a system with an inherent tendency toward scramble competition, because high consumer abundance reduces resource availability for the entire consumer population. Second, we consider a system where consumer overabundance leads to consumer starvation but not to resource damage: $d_c \equiv d$, $d_r = 0$. This represents a system with an inherent tendency toward contest competition, because high consumer abundance has no effect on resource availability for those consumers that survive starvation. These two scenarios represent "bookends" on the range of dynamics that might occur in the types of plant-insect systems that we consider; other scenarios, with differing rates of or thresholds for resource degradation versus consumer starvation, are explored in section I of Supplemental Information, available online.

Analytical Approximation

An analytical approximation is possible if we assume (1) that loss rates can be approximated as step functions ($x \to \infty$ in eqq. [4a], [4b]), (2) that density-independent death rates are close to 0 ($\alpha_c \approx 0$, $\alpha_r \approx 0$), and (3) that emergence functions can be reasonably approximated as square pulses. Under these assumptions, the emergence functions become

$$g_c(t, \theta_c) = \begin{cases} 0 & t < t_{c0} \text{ or } t > t_{cf}, \\ \dfrac{1}{\ell_c} & t_{c0} < t < t_{cf}, \end{cases} \quad (5a)$$

$$g_r(t, \theta_r) = \begin{cases} 0 & t < t_{r0} \text{ or } t > t_{rf}, \\ \dfrac{1}{\ell_r} & t_{r0} < t < t_{rf}, \end{cases} \quad (5b)$$

where t_{c0}, t_{cf}, and $\ell_c = t_{cf} - t_{c0}$ are, respectively, the start, end, and length of the consumer emergence period, while t_{r0}, t_{rf}, and $\ell_r = t_{rf} - t_{r0}$ are, likewise, the start, end, and length of the resource emergence period. Similarly, the function for consumer starvation becomes

$$h(C, R) = \begin{cases} 0 & \dfrac{C}{R} < L_T, \\ d_c C & \dfrac{C}{R} > L_T, \end{cases} \quad (6a)$$

and the function for resource loss becomes

$$m(C, R) = \begin{cases} 0 & \dfrac{C}{R} < L_T, \\ d_r R & \dfrac{C}{R} > L_T, \end{cases} \quad (6b)$$

where L_T is the critical consumer load per plant that marks the onset of consumer starvation and/or resource damage (assuming equal thresholds for both processes). As stated above, we will focus on two limiting scenarios: (1) concomitant consumer starvation and resource degradation ($d_c = d_r \equiv d$), hereafter referred to as "scenario 1," and (2) consumer starvation with no loss in resource availability ($d_c = d$, $d_r = 0$), hereafter referred to as "scenario 2." These two extremes provide a good overview of the possible types of dynamics that might be associated with our model.

Summary of Analysis Methods

Our overall approach is to use within-season models to derive discrete-time recursion relationships that map the surviving consumer population at the end of one year to the emerging consumer population at the beginning of the next. Because our within-season models capture phenology, this means that we can extrapolate from phenology change to changes in the shapes of recursion relationships. Ultimately, this enables a mechanistic interpretation of the effect of phenology on consumer dynamics and permits definition of phenological bounds on regions of parameter space featuring qualitatively different consumer dynamics.

Results

Recursion Relationships

Unless stated otherwise, we restrict our attention to systems where consumer and resource emergences are similar, both in duration and in the shapes of their respective

probability density functions (but see Supplemental Information, sec. A). Ultimately, this means that our primary focus is on the displacement between consumer and resource emergences.

Analytical Model. For consumer and resource emergence periods of equal length, $\ell_c = \ell_r \equiv \ell$. Under this assumption, $t_{r0} - t_{c0} = t_{rf} - t_{cf} \equiv \Delta$, where Δ is a measure of the onset of resource emergence relative to the onset of consumer emergence (i.e., relative phenology). When $\Delta < 0$, consumer emergence begins after resource emergence. In contrast, when $\Delta > 0$, consumer emergence begins before resource emergence. Four qualitatively different regimes are possible: (1) consumer emergence occurs fully before resource emergence ($0 < \ell < \Delta$), (2) consumer emergence occurs partially before resource emergence ($0 < \Delta < \ell$), (3) resource emergence occurs partially before consumer emergence ($-\ell < \Delta < 0$), and (4) resource emergence occurs fully before consumer emergence ($\Delta < -\ell < 0$). These regimes are outlined in figure 1. As illustrated, we assume that the consumer life span extends well beyond the consumer and resource emergence periods ($t_f \gg t_{cf}$ and $t_f \gg t_{rf}$).

Figure 2a shows scenario 1 (i.e., consumer starvation occurs concomitantly with resource degradation: $d_c = d_r \equiv d$) recursion relationships for the analytical model (eqq. [1], [2], [5], [6]; Supplemental Information, sec. A) for each of the four phenology regimes. Broadly speaking, all curves in Fig. 2a are hump shaped, with a sudden drop in consumer survival at some critical consumer density—a form of recursion relationship reminiscent of Ricker-type models. Phenology is important because it alters both the initial slope of the recursion relationship and the critical consumer density associated with population collapse. In particular, when consumers emerge earlier, the initial slope of the recursion
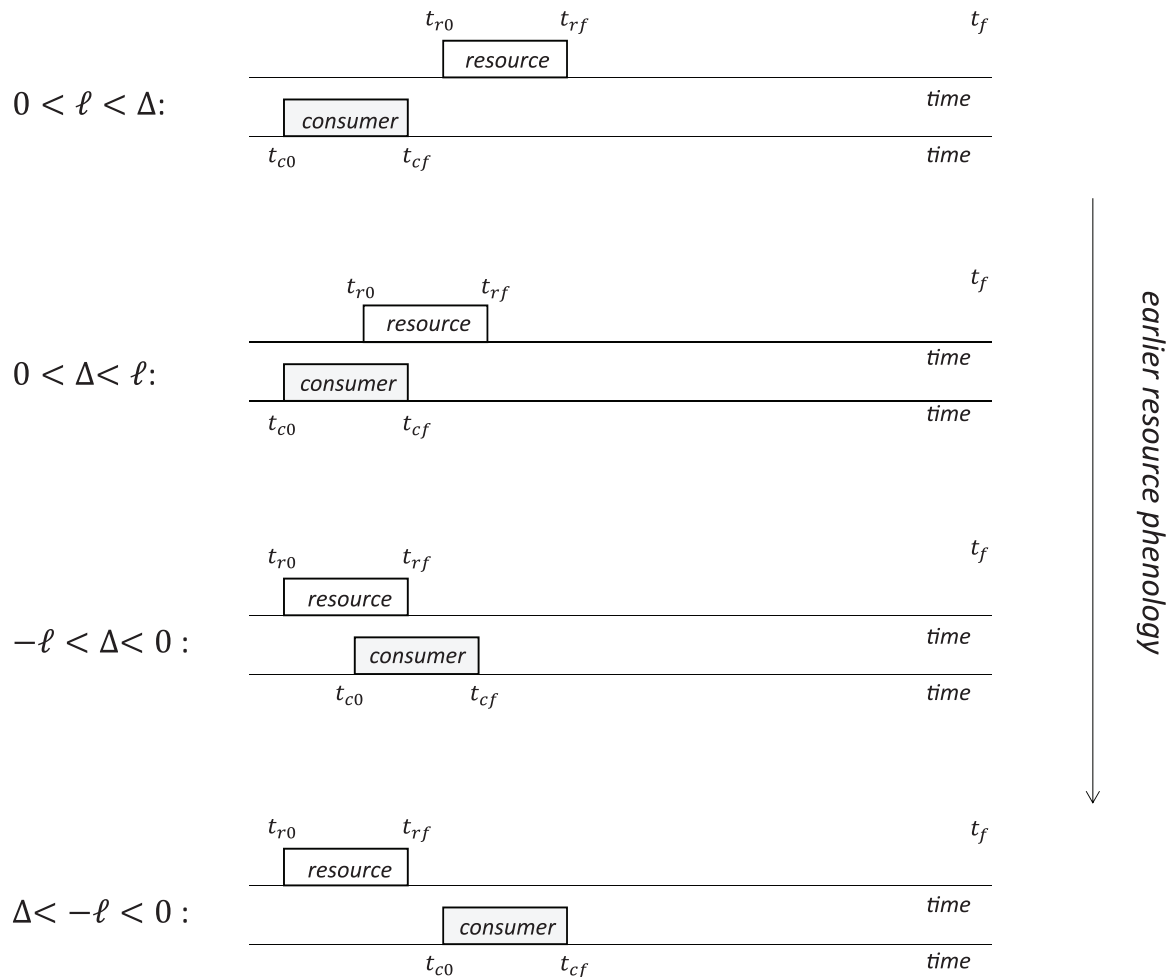
Figure 1: Qualitatively different scenarios for consumer and resource emergence. Blocks denote emergence periods only and not activity windows, which are determined by the interplay between emergence and loss.
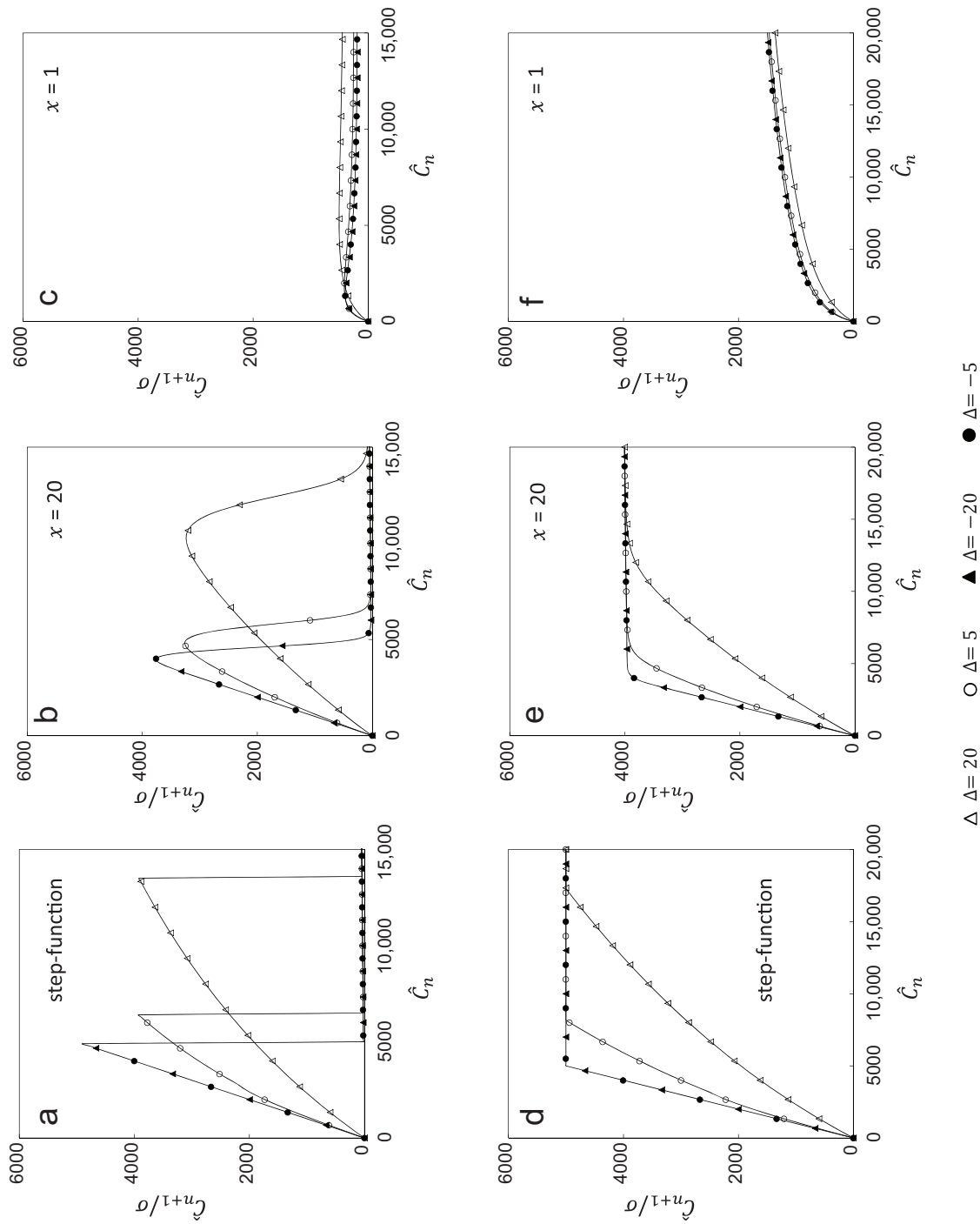
Figure 2: Recursion relationships for scenario 1 ($d_c = d_r \equiv d = 0.05$) analytical models ($a$; eqq. [A.1.6], [A.2.5], and [A.3.5] in Supplemental Information, available online), scenario 2 ($d_c = 0.05$, $d_r = 0$) analytical models (d; eqq. [F.1.6], [F.2.5], and [F.3.8] in Supplemental Information), scenario 1 ($d_c = d_r \equiv d = 0.05$) full models ($b, c$; substituting eqq. [3], [4a], and [4b]) into eq. [1]), and scenario 2 ($d_c = 0.05$, $d_r = 0$) full models (e, f; substituting eqq. [3], [4a], and [4b] into eq. [1]). In all panels, $t_t = 150$ and $\hat{R} = 1,000$. In a and d, $L_T = 5$, $\ell = 10$, $t_{cf} = 40$, and $\Delta = 20$ (open triangles), 5 (open circles), -5 (filled circles), or -20 (filled triangles). In b, c, e, and f, $\lambda_c = \lambda_r = 1$; $\phi_c = \phi_r = 10$; $\delta = 1 \times 10^{-10}$; $\alpha_c = \alpha_r = 0$; $\varepsilon_c = 26$; $\varepsilon_r = 46$ (open triangles), 31 (open circles), 21 (filled circles), or 6 (filled triangles); and (b, e) $K = 5^{20}$ and $x = 20$ or (c, f) $K = 5$ and $x = 1$. Curves with resource emerging first are identical; thus, in each panel, the curve with filled circles is superimposed on the curve with filled triangles. For the case of synchronous consumer and resource emergence, see Supplemental Information, section J.

relationship is smaller and the drop in consumer survival occurs at higher consumer densities.

Figure 2*d* shows scenario 2 (i.e., there is no resource degradation: $d_c \equiv d$, $d_r = 0$) recursion relationships for the analytical model (eqq. [1], [2], [5], [6]; Supplemental Information, sec. F) for each of the four phenology regimes. In this case, all curves are saturating, which is more reminiscent of Beverton-Holt-type models. Again, phenology is important because it alters both the initial slope of the recursion relationship and the consumer density at which saturation occurs. More specifically, when consumers emerge earlier, the initial slope of the recursion relationship is smaller, and the onset of consumer saturation occurs at higher consumer densities.

Table 1 summarizes the primary effects of phenology on the slopes and population collapse/saturation points for scenario 1 and scenario 2 recursion relationships. Comparing results from the two different scenarios suggests that the effects of phenology are similar, regardless of the assumptions made regarding resource degradation. Most notably, the initial slopes of the recursion relationships for the two scenarios are identical, indicating that thresholds for extinction should be independent of resource degradation assumptions.

Full Model. Figures 2*b*, 2*c*, 2*e*, and 2*f* show recursion relationships for the full model (eqq. [1]–[4]) with gamma function emergence rates and Hill function loss rates. To compare these results directly to the analytical model, we have set $K = L_T^x$. This fixes the inflection points for m and h in the full model (eqq. [4a], [4b]) to the threshold C/R ratio in the analytical model (eqq. [6]). Similarly, we have selected values of λ and ϕ that yield gamma distributions (eqq. [3]) with a width at one-quarter maximum height equal to the length of the emergence windows (ℓ) in the analytical model. We have also set $\alpha_c = \alpha_r = 0$ (but see fig. S9 in Supplemental Information, sec. I). Likewise, we have assumed a value for ε_c that sets the timing of the maximum in the consumer emergence function equal to the half-way point of the consumer emergence period in the analytical model (note that the correlation between models will not be perfect, because the gamma distribution is asymmetric about its maximum). Finally, we have picked ε_r values corresponding to the Δ values considered in the analytical model. Specifically, we have defined $\Delta = \varepsilon_r - \varepsilon_c$ in the full model, which corresponds to $\Delta = t_{r0} - t_{c0} = t_{rf} - t_{cf}$ in the analytical model.

As compared to the analytical model, the full model assumes smoother emergence functions and smoother increases in consumer and resource death as a function of consumer abundance. Not unexpectedly, this has the effect of smoothing out recursion relationships. In addition, recursion relationships from the full model exhibit lower maximum survival, as compared to the analytical model. This becomes increasingly apparent at low values of x and is a direct result of increased consumer and resource death at low consumer abundance when x is small. Aside from these differences, the analytical model and the full model make similar predictions.

Population Dynamics

Three qualitatively different dynamics are possible: (1) the consumer population may become extinct (E), (2) the consumer population may reach an equilibrium size (S), and (3) the consumer population may exhibit oscillatory or chaotic dynamics (C; for a discussion of oscillations versus chaos, see Supplemental Information, sec. E). Importantly, well-established theory maps each of these different dynamic outcomes to the particular shape of a population's recursion relationship (see Supplemental Information, sec. B). This simple interpretation of population dynamics is what motivated us to recast consumer-resource phenology as a transformation to the shape of the consumer recursion relationship (see "Recursion Relationships").

Table 1: The effect of phenology Δ on the initial slope of the recursion relationship and the location of population collapse or saturation for scenarios 1 and 2

Scenario, consumer emergence	Initial slope	Collapse (scenario 1)/ Saturation (scenario 2)
Scenario 1:[a]		
Fully before resource ($0 < \ell < \Delta$)	$(e^{d\ell} - 1)/(e^{d\Delta}d\ell)$	$\hat{C}/\hat{R} = L_T e^{d\Delta}$
Partially before resource ($0 < \Delta < \ell$)	$1 + [(1 - e^{-d\Delta} - d\Delta)/(d\ell)]$	$\hat{C}/\hat{R} = L_T e^{d\Delta}$
After resource ($\Delta < 0$)	1	$\hat{C}/\hat{R} = L_T$
Scenario 2:[b]		
Fully before resource ($0 < \ell < \Delta$)	$(e^{d\ell} - 1)/(e^{d\Delta}d\ell)$	$\hat{C}/\hat{R} = L_T e^{d\Delta}[d\ell/(1 - e^{-d\ell})]$
Partially before resource ($0 < \Delta < \ell$)	$1 + [(1 - e^{-d\Delta} - d\Delta)/(d\ell)]$	$\hat{C}/\hat{R} = L_T e^{d\Delta}[d\ell/(1 - e^{-d\ell})]$
After resource ($\Delta < 0$)	1	$\hat{C}/\hat{R} = L_T$

[a] Scenario 1 is the model with concomitant consumer starvation and resource degradation; see Supplemental Information, available online, section A.

[b] Scenario 2 is the model with only consumer starvation but no loss of resource; see Supplemental Information, section F.

Table 2: Phenology ranges that yield each of the qualitatively different consumer dynamics for scenarios 1 and 2

Scenario, consumer emergence	Extinction	Equilibrium	Oscillations/chaos
Scenario 1:[a]			
Fully before resource $(0 < \ell < \Delta)$	$\Delta > d^{-1}\ln(\sigma(1 - e^{-d\ell})/(d\ell)) + \ell$	$d^{-1}\ln(\sigma(1 - e^{-d\ell})/(d\ell)) + \ell > \Delta > d^{-1}\ln(\sigma(1 - e^{-d\ell})/(d\ell))$	$\Delta < d^{-1}\ln(\sigma(1 - e^{-d\ell})/(d\ell))$
Partially before resource $(0 < \Delta < \ell)$	$\Delta > d^{-1}[W(-e^{(d\ell/\sigma)-d\ell-1}) + 1 - (d\ell/\sigma)] + \ell$	$d^{-1}[W(-e^{(d\ell/\sigma)-d\ell-1}) + 1 - (d\ell/\sigma)] + \ell > \Delta > d^{-1}\ln(\sigma(1 - e^{-d\ell})/(d\ell))$	$\Delta < d^{-1}\ln(\sigma(1 - e^{-d\ell})/(d\ell))$
After resource $(\Delta < 0)$	Never	Never	Always
Scenario 2:[b]			
Fully before resource $(0 < \ell < \Delta)$	$\Delta > d^{-1}\ln(\sigma(1 - e^{-d\ell})/(d\ell)) + \ell$	$\Delta < d^{-1}\ln(\sigma(1 - e^{-d\ell})/(d\ell)) + \ell$	Never
Partially before resource $(0 < \Delta < \ell)$	$\Delta > d^{-1}[W(-e^{(d\ell/\sigma)-d\ell-1}) + 1 - (d\ell/\sigma)] + \ell$	$\Delta < d^{-1}[W(-e^{(d\ell/\sigma)-d\ell-1}) + 1 - (d\ell/\sigma)] + \ell$	Never
After resource $(\Delta < 0)$	Never	Always	Never

Note: W denotes the Lambert W function.
[a] Scenario 1 is the model with concomitant consumer starvation and resource degradation; see Supplemental Information, available online, section B.
[b] Scenario 2 is the model with only consumer starvation but no loss of resource; see in Supplemental Information, section G.

To extrapolate from the effects of phenology on the recursion relationship to specific implications for population dynamics, we use two approaches. First, we use the analytical model to define phenology ranges bounding qualitatively different consumer dynamics. By doing this, we can examine the role of different model parameters on overall consumer response to phenology change. Second, we use numerical solution of the full model to construct orbit diagrams. These are standard tools for visualizing the behavior (phase space) of discrete-time dynamical systems, and they allow us to compare full-model results with analytical predictions.

Table 2 outlines the phenology ranges predicted by the analytical model for each of the three different types of population dynamics (extinction, equilibrium, and oscillations/chaos). Not unexpectedly, chaotic dynamics are possible only in scenario 1, where the initial recursion relationship resembles that of a Ricker model. In scenario 2, where the recursion relationship more closely resembles a Beverton-Holt model, only extinction and equilibrium dynamics are possible. In both scenarios, shifts in resource phenology can result in qualitative changes in consumer dynamics. In scenario 1, consumer extinction occurs when consumer emergence begins long before resource emergence (large positive

Table 3: Observable consumer population dynamics for each of the different emergence scenarios as a function of consumer fecundity

Scenario, fecundity	Mathematical description	Consumers emerge first		Resource emerges first
		Fully $(0 < \ell < \Delta)$	Partially $(0 < \Delta < \ell)$	$(\Delta < 0)$
Scenario 1:				
High	$\sigma > d\ell e^{d\ell}/(1 - e^{-d\ell})$	Extinction (E), equilibrium (S) oscillations/chaos (C)	Oscillations/chaos (C)	Oscillations/chaos (C)
Intermediate	$d\ell/(1 - e^{-d\ell}) < \sigma < d\ell e^{d\ell}/(1 - e^{-d\ell})$	Extinction (E), equilibrium (S)	Equilibrium (S), oscillations/chaos (C)	Oscillations/chaos (C)
Low	$\sigma < d\ell/(1 - e^{-d\ell})$	Extinction (E)	Extinction (E), equilibrium (S)	Oscillations/chaos (C)
Scenario 2:				
High	$\sigma > d\ell/(1 - e^{-d\ell})$	Extinction (E), equilibrium (S)	Equilibrium (S)	Equilibrium (S)
Low	$\sigma < d\ell/(1 - e^{-d\ell})$	Extinction (E)	Extinction (E), equilibrium (S)	Equilibrium (S)

Note: See figure 1 for the emergence scenarios. Also see Supplemental Information, available online, sections C and I.
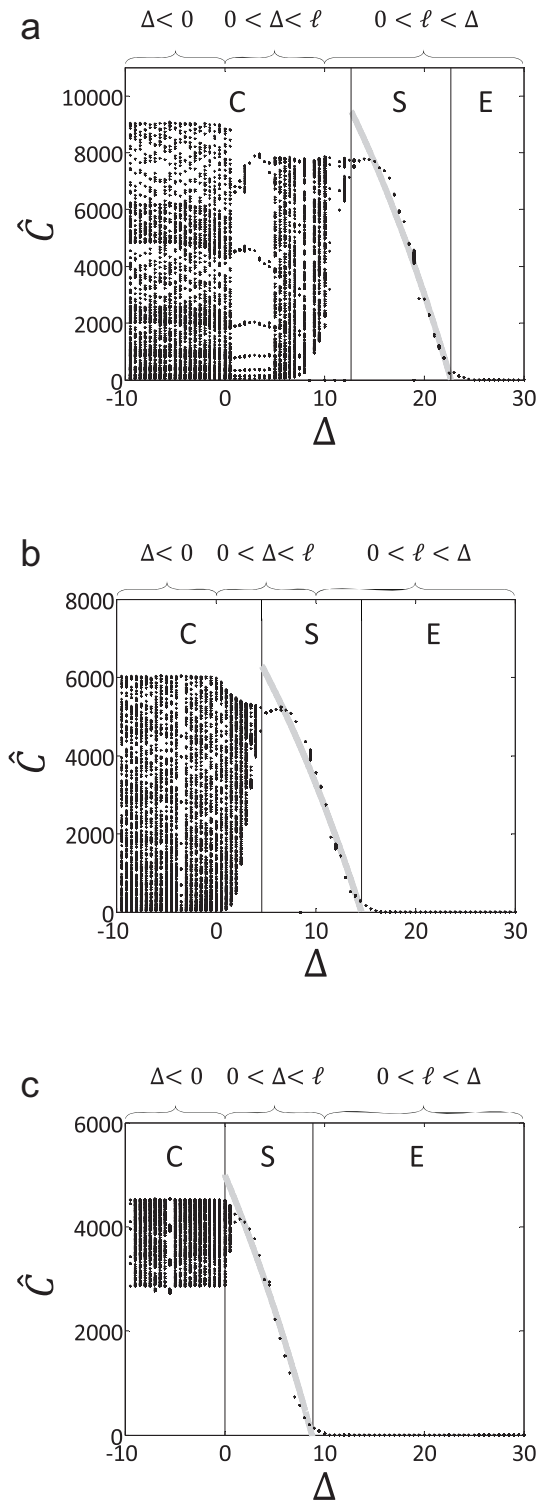
Figure 3: Orbit diagrams for scenario 1, showing consumer dynamics in the full model as a function of $\Delta = \varepsilon_r - \varepsilon_c$ for systems with high (*a*), intermediate (*b*), and low (*c*) consumer fecundity. In each panel, the labels denote regions predicted to exhibit qualitatively different dynamics—specifically, oscillations/chaos (C), an equilibrium popula-
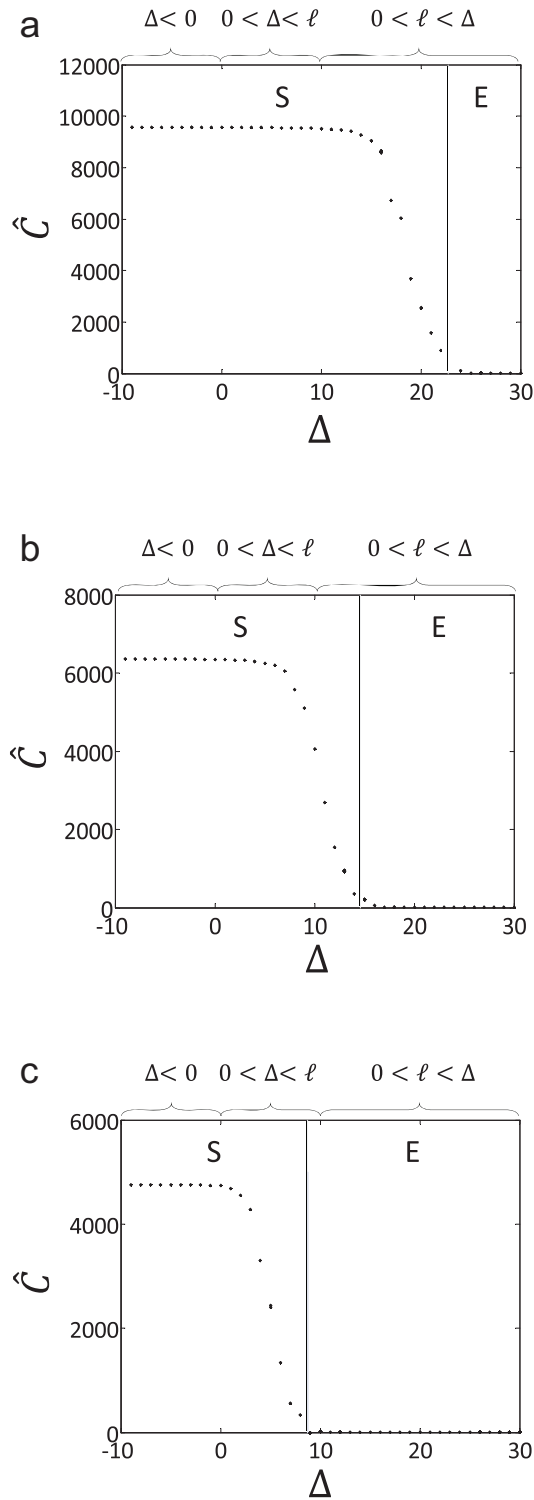
Δ), an equilibrium consumer population occurs when consumer emergence begins only slightly before resource emergence (intermediate Δ), and consumer oscillations or chaos occur when consumer emergence begins nearly coincident with or after resource emergence (both small positive Δ and negative Δ). In scenario 2, predictions are similar, with identical boundaries between extinction and equilibrium dynamics but no oscillatory or chaotic regions. Biologically speaking, this suggests that relatively later resource phenology can result in consumer extinction, whereas relatively earlier resource phenology can result in oscillatory or chaotic consumer population dynamics, with oscillations and chaos possible only in systems that have inherently Ricker-like recursion relationships.

Although phenology is an important determinant of consumer dynamics, dynamics can also be affected by consumer fecundity. Thus, the phenology ranges in Table 2 depend on σ. In scenario 1, for example, high consumer fecundity (large σ) increases the boundary on oscillations/chaos, $\Delta < d^{-1}\ln(\sigma(1 - e^{-d\ell})/(d\ell))$. As a result, highly fecund consumer populations can exhibit oscillatory/chaotic dynamics even when these consumers emerge quite early relative to their resource (i.e., even at fairly large Δ). By contrast, in both scenario 1 and scenario 2, low fecundity (small σ) decreases the boundary on extinction, $\Delta > d^{-1}\ln(\sigma(1 - e^{-d\ell})/(d\ell)) + \ell$ or $\Delta > d^{-1}(\text{Lambert } W(-e^{d\ell/\sigma - d\ell - 1}) + 1 - d\ell/\sigma) + \ell$. Consequently, consumers with low fecundity may become extinct even if they emerge only slightly ahead of their resource (i.e., even at fairly small Δ). Consistent with the role that fecundity plays in determining phenological bounds on consumer dynamics, we find that, depending on specific fecundity thresholds, only certain consumer population dynamics are possible for each different phenology regime (fig. 1). Table 3 outlines analytical predictions for these fecundity thresholds.

Figures 3 (scenario 1) and 4 (scenario 2) compare predictions from the analytical model (tables 2, 3) to orbit diagrams from the full model with $x = 20$. As above, we define $\Delta = \varepsilon_r - \varepsilon_c$ as our measure of phenology in the full model, which corresponds to $\Delta = t_{r0} - t_{c0} = t_{rf} - t_{cf}$ in the analytical model. In Figures 3 and 4, the regions labeled oscillations/chaos (C), equilibrium population size (S), and population extinction (E) are determined on the basis of the analytical range predictions in table 2. Note that these

tion size (S), and population extinction (E)—according to the analytical model. The gray line represents the equilibrium population size as predicted by the analytical model (eqq. [B.1.14.d] and [B.2.18.d] in Supplemental Information, available online). Corresponding parameters are $\delta = 1 \times 10^{-10}$, $\alpha_c = \alpha_r = 0$, $K = 5^{20}$, $x = 20$, $\phi_c = \phi_r = 10$, $\lambda_c = \lambda_r = 1$, and $\varepsilon_c = 26$ for the full model and $L_T = 5$ and $\ell = 10$ for the analytical model. For both the full and analytical models, we assume $d_c = d_r \equiv d = 0.05$, $t_f = 150$, $\hat{R} = 1{,}000$, and a net fecundity σ of 2.4 (high; *a*), 1.6 (medium; *b*), or 1.2 (low; *c*).

Figure 4: Orbit diagrams for scenario 2, showing consumer dynamics in the full model as a function of $\Delta = \varepsilon_r - \varepsilon_c$ for systems with high (*a*), intermediate (*b*), and low (*c*) consumer fecundity. In each panel, the labels denote regions predicted to exhibit qualitatively different dynamics—specifically, an equilibrium population size (S) and population extinction (E)—according to the analytical model. Corresponding parameters are $\delta = 1 \times 10^{-10}$, $\alpha_c = \alpha_r = 0$, $K = 5^{20}$, $x = 20$, $\phi_c = \phi_r = 10$, $\lambda_c = \lambda_r = 1$, and $\varepsilon_c = 26$ for the full model and $L_T = 5$ and $\ell = 10$ for the analytical model. For both the full and analytical models, we assume $d_c \equiv d = 0.05$, $d_r = 0$, $t_f = 150$, $\hat{R} = 1{,}000$, and a net fecundity σ of 2.4 (high; *a*), 1.6 (medium; *b*), or 1.2 (low; *c*).
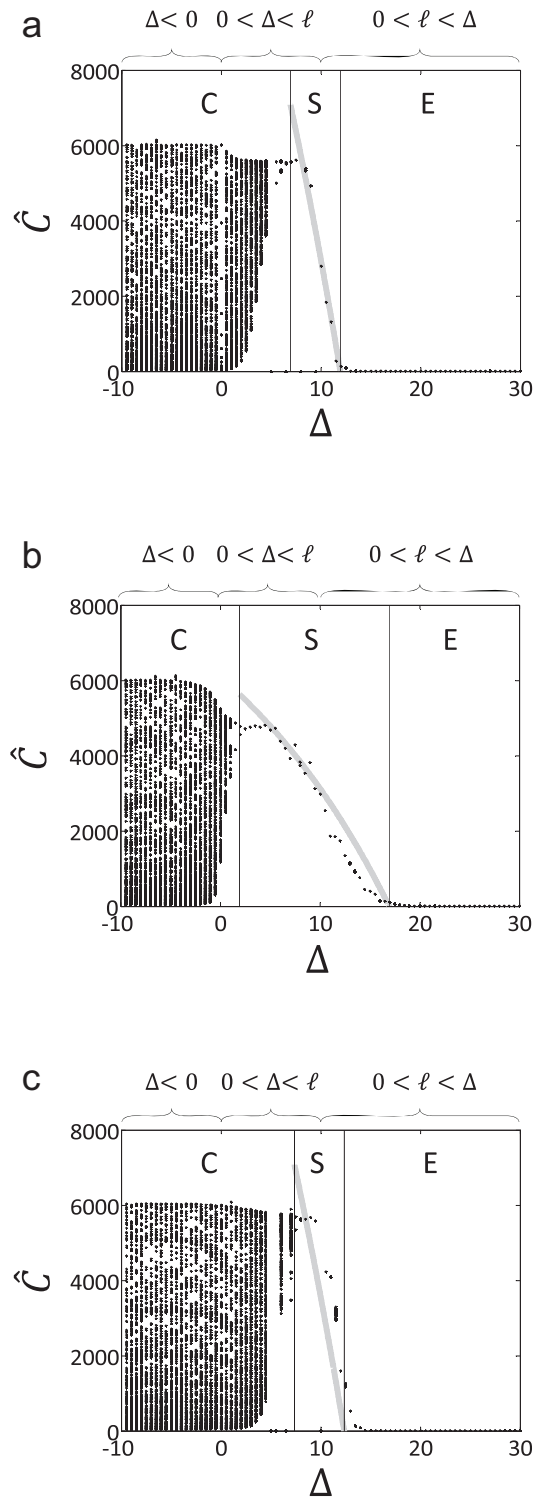
regions align almost perfectly with the orbit diagrams; thus, positive consumer abundances first appear in the orbit diagrams very near the predicted S-E boundaries, while oscillations/chaos first appear very near the predicted C-S boundaries. This suggests that the analytical ranges in table 2 are good approximations for the same ranges in the full model, at least for large x (i.e., consumer overdispersion).

To compare predictions from table 3 to the orbit diagrams in figures 3 and 4, we contrast figures with differing consumer fecundities. When consumer fecundity is high, for example, consumer emergence fully before resource emergence ($0 < \ell < \Delta$) can lead to C, S, or E dynamics in scenario 1 (fig. 3*a*) and S or E dynamics in scenario 2 (fig. 4*a*). At intermediate consumer fecundity, however, this same phenology regime can give only S or E dynamics, even in scenario 1 (figs. 3*b*, 4*b*). Finally, at low consumer fecundity, consumer emergence fully before resource emergence always results in consumer extinction (figs. 3*c*, 4*c*). These results are fully consistent with the predictions made in table 3, suggesting, once again, that the analytical model broadly captures the behavior of the full model when consumers are overdispersed (large x).

In addition to fecundity, the durations of the consumer and resource emergence periods are also important in determining qualitative dynamics. However, to fully understand the role of the emergence period, it is necessary to consider potentially different emergence durations for the consumer and the resource. In the analytical model, this means assuming potentially different ℓ_c and ℓ_r; in the full model, it means assuming potentially different θ_c and θ_r. To define a phenology metric for the analytical model, we use the time difference between the midpoints of the emergence windows, $\Delta' = t_{r0} + \ell_r/2 - t_{c0} - \ell_c/2 = t_{rf} - \ell_r/2 - t_{cf} + \ell_c/2$. To define a comparable phenology metric for the full model, we use $\Delta' = t_{r,max} - t_{c,max}$, where $t_{r,max}$ and $t_{c,max}$ are the times that maximize resource and consumer emergence, respectively.

Figure 5 (also see fig. S5 in Supplemental Information) shows analytical range boundaries (see Supplemental Information, sec. A) and full-model orbit diagrams for systems with variable consumer and resource emergence periods. All else being equal, longer resource emergence periods result in the onset of oscillations/chaos (i.e., the C-S boundary) at smaller Δ (scenario 1 only) and the onset of extinction (i.e., the S-E boundary) at larger Δ (both scenario 1 and scenario 2; Supplemental Information, sec. D). Importantly,

this means that a wider range of resource phenologies give rise to equilibrium consumer dynamics (compare, e.g., figs. 5*a* and 5*b*). In contrast, longer consumer emergence periods result in the onset of oscillations/chaos (i.e., the C-S boundary) at larger Δ (scenario 1 only) and, except at low fecundity, the onset of extinction (i.e., the S-E boundary), also at larger Δ (both scenario 1 and scenario 2; Supplemental Information, sec. D). Consequently, the length of the consumer emergence window has little to no effect on the range of resource onset dates that give equilibrium consumer population dynamics. However, for longer consumer emergence windows, there is a small shift of this entire range to later resource dates overall (compare, e.g., figs. 5*a* and 5*c*).

One benefit of the full model is that it can be used to examine systems with a more gradual onset of consumer starvation and/or resource degradation (small *x*) as a function of consumer density. As suggested above, this is consistent with consumers that have a more clustered distribution across host plants. Figure 6 (see also fig. S6 in Supplemental Information, sec. I) shows orbit diagrams for a system with a moderate threshold response ($x = 5$) and a system with a saturating response ($x = 1$). Comparing these orbit diagrams to the C, S, and E range boundaries predicted by the analytical model (also shown in fig. 6) suggests that, in the case of small *x*, the predictions of the analytical model and the full model are markedly different, particularly at small or negative Δ. For example, in the system with $x = 5$ (fig. 6*a*), the analytically predicted C-S boundary occurs at larger Δ than is actually observed in the orbit diagram. Meanwhile, in the system with $x = 1$ (fig. 6*b*), the orbit diagram fails to exhibit oscillations/chaos at all. This latter result should not be surprising, since the recursion relationship for this model (see fig. 2*c*) does not exhibit the same sharp drop in survival that is necessary to generate oscillatory or chaotic dynamics. Despite these differences, the analytical model and the full model are in close agreement as to the level of Δ above which the consumer population is predicted to become extinct. Thus, the extinction bounds in ta-

---

(*b*), and a short resource emergence period and a long consumer emergence period (*c*). In each panel, the labels denote regions predicted to exhibit qualitatively different dynamics—specifically, oscillations/chaos (C), an equilibrium population size (S), and population extinction (E)—according to the analytical model. The gray line represents the equilibrium population size as predicted by the analytical model (eqq. [B.1.14.d] and [B.2.18.d] in Supplemental Information, available online). Corresponding parameters for the full model are $\delta = 1 \times 10^{-10}$; $\alpha_c = \alpha_r = 0$; $K = 5^{20}$; $x = 20$; $\phi_c = \phi_r = 10$; $\sigma = 1.6$; and (*a*) $\lambda_c = 2$, $\lambda_r = 2$, $\varepsilon_c = 30.5$, and $\varepsilon_r = 30.5 + \Delta'$; (*b*) $\lambda_c = 2$, $\lambda_r = 0.67$, $\varepsilon_c = 30.5$, and $\varepsilon_r = 21.6 + \Delta'$; or (*c*) $\lambda_c = 0.67$, $\lambda_r = 2$, $\varepsilon_c = 21.6$, and $\varepsilon_r = 30.5 + \Delta'$. For the analytical model, we assume $L_T = 5$, $\sigma = 1.6$, $\Delta' = t_{r0} + (\ell_r/2) - t_{c0} - (\ell_c/2)$, and (*a*) $\ell_c = 5$ and $\ell_r = 5$, (*b*) $\ell_c = 5$ and $\ell_r = 15$, or (*c*) $\ell_c = 15$ and $\ell_r = 5$. For both the analytical model and the full model, we assume $d_c = d_r \equiv d = 0.05$, $t_f = 150$, and $\hat{R} = 1{,}000$.
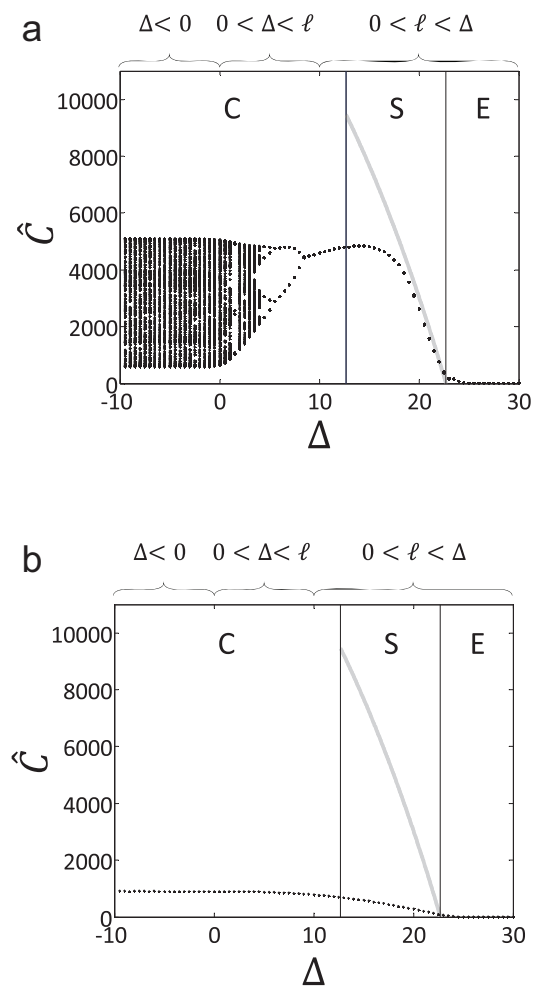
Figure 5: Orbit diagrams for scenario 1, showing consumer dynamics in the full model as a function of $\Delta' = t_{r,\max} - t_{c,\max}$ (i.e., the displacement between the maxima of the two emergence curves) for systems with short consumer and resource emergence periods (*a*), a long resource emergence period and a short consumer emergence period

a

b

Figure 6: Orbit diagrams for scenario 1 as a function of $\Delta = \varepsilon_r - \varepsilon_c$ for the full model with $d = 0.05$, $t_f = 150$, $\hat{R} = 1,000$, $\delta = 1 \times 10^{-10}$, $\alpha_c = \alpha_r = 0$, $\phi_c = \phi_r = 10$, $\lambda_c = \lambda_r = 1$, $\varepsilon_c = 26$, $\sigma = 2.4$, and (*a*) $K = 5^5$ and $x = 5$ or (*b*) $K = 5$ and $x = 1$. In each panel, the labels denote regions predicted to exhibit qualitatively different dynamics—specifically, oscillatory/chaos (C), an equilibrium population size (S), and population extinction (E)—according to the analytical model. The gray line represents the equilibrium population size as predicted by the analytical model (eqq. [B.1.14.d] and [B.2.18.d] in Supplemental Information, available online). For the analytical model, we assume $d_c = d_r \equiv d = 0.05$, $\hat{R} = 1,000$, $L_T = 5$, $\sigma = 2.4$, and $\ell = 10$.

ble 2 are still relevant, even when consumers exhibit a more clustered distribution across host plants.

Discussion

Ample evidence demonstrates that ongoing climate change is altering species phenologies worldwide (Parmesan 2006, 2007; Thackeray et al. 2010), likely as a result of temperature effects on development (Amarasekare and Savage 2012). However, the consequences of phenological change on spe-

cies abundances and species population dynamics remain poorly understood. This is particularly true in systems with interacting species (Bewick et al. 2014), especially if one species is more affected by phenological change than its partner (Miller-Rushing et al. 2010). In this article, we show that resource phenology can have profound effects on the dynamics of an obligate consumer. For example, depending on whether the consumer emerges before, during, or after resource emergence, the consumer population may become extinct, reach a fixed population size, or exhibit oscillatory and/or chaotic dynamics. These qualitatively different categories of dynamics emerge as a result of changes in phenology alone (figs. 3–5) and do not require changes in any of the underlying rate parameters. However, exactly when resource emergence must occur relative to consumer emergence so that each of these different dynamic behaviors can be observed depends on consumer and resource life-history parameters, most notably consumer fecundity and the duration of the consumer and resource emergence periods. Thus, the dynamics of different consumers may be affected differently by changing resource phenology.

Phenology as a Determinant of Intraspecific Competition

One interesting conclusion derived from our model is that phenological mismatch can alter intraspecific consumer competition in consumer-resource systems. In our system, consumers die as a result of starvation. Thus, changes in the consumer recursion relationship can be directly attributed to changes in intraspecific competition. By extension, this suggests that phenology acts by mediating intraspecific consumer competition. Traditionally, intraspecific competition has been viewed from two extremes: "contest competition" (compensatory) and "scramble competition" (overcompensatory; Bellows 1981). Scramble competition assumes equal resource partitioning and thus an abrupt change from 100% survival to 100% mortality when resources drop below the level required to maintain all consumers. In contrast, contest competition assumes that successful consumers acquire enough resource to survive and reproduce while unsuccessful consumers do not. Even at low consumer abundances, contest competition results in less than 100% survival. However, there is no abrupt drop in consumer survival as a function of consumer abundance. For most species, reality likely lies somewhere in between.

In general, systems with a steep threshold response to consumer overabundance (e.g., the analytical model with $d_c = d_r \equiv d$ or the corresponding full model with $x = 20$) inherently resemble scramble competition (i.e., sudden onset of consumer death above a specific consumer abundance). Intuitively, one might expect that this would translate into recursion relationships closely mirroring predictions for scramble competition. Such expectations are realized when

resources emerge before consumers ($\Delta < 0$). In this case, recursion relationships indicate close to 100% survival up to a critical consumer abundance and then a considerable and abrupt drop in survival above this abundance (see fig. 2*a*, 2*b*). However, when resources emerge after consumers ($\Delta > 0$), recursion relationships are characterized by less than 100% survival, even at low consumer abundances. Moreover, there is a smaller and, at least in the full model, less abrupt drop in survival going from low consumer abundance to high consumer abundance. In other words, recursion relationships for later resource emergence dates (i.e., larger Δ) begin to resemble contest competition rather than scramble competition.

These results can be explained as follows: when resources emerge partially or fully before consumers, emerging consumers have access to most ($-\ell < \Delta < 0$) or all ($\Delta < -\ell < 0$) of the total resource population. As a result, consumer survival is determined by how the consumer inherently partitions resources in the absence of phenology or phenology mismatch. The situation is different when resources emerge after consumers ($\Delta > 0$). In this case, there is initial consumer death as a result of, first, an absence of resources and, subsequently, overcrowding on the first few resource individuals that emerge (Zalucki and Suzuki 1987; Pierle 2010). Consumers that starve early in the season acquire practically none of the resource. Consumers remaining until sufficient resources have emerged, however, have plenty. This translates into recursion relationships with stronger contest-competition characteristics, even when those same consumers would partition resources equally (i.e., scramble-like) in the absence of phenology.

Consequences of Phenology for Population Dynamics

Much emphasis has been placed on the potential for extinction as a result of phenological mismatches (Cahill et al. 2013). In our consumer-resource model, this occurs when consumers emerge far ahead of the resource (large Δ). For these scenarios, the extent of consumer starvation that occurs before resource emergence is so great that sustaining a viable consumer population is impossible. In the context of climate change, early consumer emergence will occur when the phenology of the consumer population advances faster than the phenology of its resource. Although there is a paucity of long-term data on relative phenology changes among interacting species (Russell and Louda 2004; Visser and Both 2005; Parmesan 2007; Singer and Parmesan 2010), several insects have been observed or are predicted to advance faster than their host plants in response to warming conditions. For example, a number of studies have indicated that the hatching of winter moth (*Opherophtera brumata*) eggs is advancing faster than budburst on either oak (*Quercus robar*; Visser and Holleman 2001; but see Buse and Good 1996) or Sitka spruce

(*Picea sitchensis*; Dewar and Watt 1992). Similarly, red admiral butterflies (*Vanessa atalanta*) have advanced their return date to Britain over the past 2 decades, whereas the flowering of a key host plant, the stinging nettle (*Urtica dioica*), has not (Sparks et al. 2005; Visser and Both 2005). Indeed, butterfly phenology overall seems to have advanced faster than the phenology of herbs and grasses, suggesting that red admirals may be a single example of a broader pattern (Singer and Parmesan 2010). Thus, the threat of phenological mismatch for a number of Lepidoptera species may be extinction (McLaughlin et al. 2002; Singer and Parmesan 2010).

Another potential outcome of phenological mismatch that is predicted by our model is the appearance of or changes to outbreak dynamics. This outcome may be particularly relevant for certain lepidopteran pests (Moscardi 1999) that already exhibit outbreaks (van Asch and Visser 2007; Jepsen et al. 2008). Although outbreak dynamics are typically attributed to top-down mechanisms such as disease or parasitoids, recent studies have suggested that intraspecific competition may be a contributing factor (Abbott and Dwyer 2007). If this is true, our model predicts that the advancement of the pest phenology relative to its host could have the effect of dampening or even preventing outbreak dynamics. Collapsing population cycles have been documented for larch budmoth (Johnson et al. 2010) as well as a number of non-insect herbivores (Ims et al. 2008). Interestingly, in the case of larch budmoth, a detailed analysis of a spatial, tritrophic Nicholson-Bailey model indicated that mismatches between budmoths and their host were responsible for loss of outbreak dynamics (Johnson et al. 2010). While the focus of that study was on spatial mismatch, the authors pointed to mismatched phenology as another reason for the recent decrease in budmoth outbreaks.

In contrast to budmoths, a number of studies have suggested that climate change will cause an increase in outbreak intensities (Logan et al. 2003). We see this in our model when consumer phenology advances more slowly than that of its host. In this case, insect populations that exhibit equilibrium population sizes can be pushed into an oscillatory regime characteristic of outbreaks. Even in species that currently exhibit population cycles, oscillation amplitude may increase with increasingly early resource phenology. This is similar to results from parasitoid-regulated systems, although in these systems, it is the relative timing of the parasitoid, not the resource, that influences host dynamics (Umbanhowar and Hastings 2002; Cobbold et al. 2009; Moran et al. 2013). In addition to instigating or worsening outbreaks, a shift in resource phenology to relatively earlier dates may drive species from predictable outbreak cycles to chaotic outbreak cycles. Importantly, this deterministic effect is distinct from increasing climate stochasticity, which may also lead to outbreaks that are increasingly erratic. While

there are few records of insect species advancing more slowly than their hosts, a recent study suggests that insect species in general are advancing more slowly than plants (Thackeray et al. 2010). If this is true, then a large number of insect species may be at risk of moving into the "outbreaking pest" category by virtue of temporal mismatches.

Future Directions and Conclusions

Having identified the key role that phenology plays in changing the behavior of a simple consumer-resource model, it is natural to identify possible extensions that would allow for the inclusion of additional rich biological detail. One important consideration is consumer life span. In this article, we have assumed short consumer emergence periods relative to consumer life span. Reversing this assumption would lower intraspecific competition, potentially reducing the opportunity for phenology to affect consumer competition and thus consumer dynamics. Similarly, we have considered only univoltine insects. In a model that accounts for multivoltinism or even changes in voltinism (Tobin et al. 2008), different consumer generations would experience resource phenology at different time points throughout the season (and thus at different levels of availability). In this case, year-to-year recursion relationships would reflect the compound effects of all generations, possibly minimizing the role of early-season starvation. Likewise, we have generally assumed that all resource individuals not killed by overgrazing remain available until the end of the consumer life span (but see fig. S10 in Supplemental Information, sec. I). Shorter resource life spans could reflect short-lived plants or plants that become less palatable as they mature. This would alter predictions for scenarios with early resource emergence where premature resource senescence could ultimately result in consumer starvation toward the end of the consumer life span. Finally, all of our models of phenology change have assumed an a priori level of phenological mismatch. If this is associated with a more mechanistic underpinning—for example, by relating phenology and potentially other life-history parameters of individual species directly to temperature (Vasseur and McCann 2005; Petchey et al. 2010; Amarasekare and Savage 2012; Dell et al. 2014) and then embedding these parameters into a similar model—it would be possible to arrive at a more direct relationship between measurable abiotic factors and biotic outcomes (for an example of how this might be done, see fig. S11 in Supplemental Information, sec. I).

All of the extensions listed above would increase system complexity. Our model, however, highlights the fact that even simple systems with straightforward species interactions can exhibit complex and nonintuitive responses to changes in phenology. For consumer-resource systems, the most dramatic effects occur in systems with short resource emergence periods. In these systems, there is a reduction in the range of phenologies that give rise to equilibrium population dynamics. As a result, systems with short resource emergence periods may be more susceptible to small perturbations in resource phenology. Of course, whether a plant has a short or a long emergence period will depend on the trade-offs faced by the plant, and these may, in turn, influence the plant's response to climate change. A long emergence period can be a bet-hedging strategy that allows the plant population to survive in an unpredictable environment (Post et al. 2001). On the other hand, a long emergence period can put a small population at risk of an Allee effect (Calabrese and Fagan 2004). This may be particularly severe in small plant populations with a short flowering window tied closely to the emergence period of a pollinator (Fagan et al. 2014). The effects of resource phenology are also particularly important for consumer species that would exhibit strong scramble competition in the absence of phenology. For these species, small shifts in the timing of resource emergence can have large impacts on the type of intraspecific competition that the consumer population experiences.

While the importance of phenology effects depends on consumer and resource life-history traits as well as on the magnitudes of the phenology changes experienced, our study has shown that a wide range of perturbations to species phenologies can disrupt consumer-resource interactions. At the very least, such phenological shifts result in altered consumer population abundances. Often, however, these shifts fundamentally redefine consumer population dynamics, tipping populations toward extinction at one end and chaos at the other.

Literature Cited

Abbott, K. C., and G. Dwyer. 2007. Food limitation and insect outbreaks: complex dynamics in plant-herbivore models. Journal of Animal Ecology 76:1004–1014.

Amarasekare, P., and V. Savage. 2012. A framework for elucidating the temperature dependence of fitness. American Naturalist 179: 178–191.

Bale, J. S., G. J. Masters, I. D. Hodkinson, C. Awmack, T. M. Bezemer, V. K. Brown, J. Butterfield, et al. 2002. Herbivory in global climate change research: direct effects of rising temperature on insect herbivores. Global Change Biology 8:1–16.

Bellows, T. S. 1981. The descriptive properties of some models for density dependence. Journal of Animal Ecology 50:139–156.

Bewick, S., K. L. Stuble, J. P. Lessard, R. R. Dunn, F. R. Adler, and N. J. Sanders. 2014. Predicting future coexistence in a North American ant community. Ecology and Evolution 4:1804–1819.

Both, C., M. van Asch, R. G. Bijlsma, A. B. van den Burg, and M. E. Visser. 2009. Climate change and unequal phenological changes across four trophic levels: constraints or adaptations? Journal of Animal Ecology 78:73–83.

Broberg, C. L., J. H. Borden, and L. M. Humble. 2002. Distribution and abundance of *Cryptorhynchus lapathi* on *Salix* spp. in British Columbia. Canadian Journal of Forest Research 32:561–568.

Brown, D. G., and A. E. Weis. 1995. Direct and indirect effects of prior grazing of goldenrod upon the performance of a leaf beetle. Ecology 76:426–436.

Buse, A., and J. Good. 1996. Synchronization of larval emergence in winter moth (*Operophtera brumata* L.) and budburst in pedunculate oak (*Quercus robur* L.) under simulated climate change. Ecological Entomology 21:335–343.

Cahill, A. E., M. E. Aiello-Lammens, M. C. Fisher-Reid, X. Hua, C. J. Karanewsky, H. Yeong Ryu, G. C. Sbeglia, et al. 2013. How does climate change cause extinction? Proceedings of the Royal Society B: Biological Sciences 280:20121890. doi:10.1098/rspb.2012.1890.

Calabrese, J. M., and W. F. Fagan. 2004. Lost in time, lonely, and single: reproductive asynchrony and the Allee effect. American Naturalist 164:25–37.

Calabrese, J. M., L. Ries, S. F. Matter, D. M. Debinski, J. N. Auckland, J. Roland, and W. F. Fagan. 2008. Reproductive asynchrony in natural butterfly populations and its consequences for female matelessness. Journal of Animal Ecology 77:746–756.

Cobbold, C. A., J. Roland, and M. A. Lewis. 2009. The impact of parasitoid emergence time on host-parasitoid population dynamics. Theoretical Population Biology 75:201–215.

Crawley, M. J. 1989. Insect herbivores and plant population dynamics. Annual Review of Entomology 34:531–562.

Cushing, D. H. 1990. Plankton production and year-class strength in fish populations: an update of the match/mismatch hypothesis. Pages 249–293 *in* J. H. S. Blaxter and A. J. Southward, eds. Advances in marine biology. Vol. 26. Academic Press, San Diego, CA.

Dell, A. I., S. Pawar, and V. M. Savage. 2014. Temperature dependence of trophic interactions are driven by asymmetry of species responses and foraging strategy. Journal of Animal Ecology 83:70–84.

Dewar, R. C., and A. D. Watt. 1992. Predicted changes in the synchrony of larval emergence and budburst under climatic warming. Oecologia (Berlin) 89:557–559.

Doi, H., O. Gordo, and I. Katano. 2008. Heterogeneous intra-annual climatic changes drive different phenological responses at two trophic levels. Climate Research 36:181–190.

Donnelly, A., A. Caffarra, and B. O'Neill. 2011. A review of climate-driven mismatches between interdependent phenophases in terrestrial and aquatic ecosystems. International Journal of Biometeorology 55:805–817.

Durant, J. M., D. Hjermann, G. Ottersen, and N. C. Stenseth. 2007. Climate and the match or mismatch between predator requirements and resource availability. Climate Research 33:271–283.

Fagan, W. F., S. Bewick, S. Cantrell, C. Cosner, I. G. Varassin, and D. W. Inouye. 2014. Phenologically explicit models for studying plant-pollinator interactions under climate change. Theoretical Ecology 7:289–297.

Fagan, W. F., C. Cosner, E. A. Larsen, and J. M. Calabrese. 2010. Reproductive asynchrony in spatial population models: how mating behavior can modulate Allee effects arising from isolation in both space and time. American Naturalist 175:362–373.

Forrest, J., and A. J. Miller-Rushing. 2010. Toward a synthetic understanding of the role of phenology in ecology and evolution. Philo-

sophical Transactions of the Royal Society B: Biological Sciences 365:3101–3112.

Harrington, R., I. Woiwod, and T. Sparks. 1999. Climate change and trophic interactions. Trends in Ecology and Evolution 14:146–150.

Ims, R. A., J.-A. Henden, and S. T. Killengreen. 2008. Collapsing population cycles. Trends in Ecology and Evolution 23:79–86.

Jepsen, J. U., S. B. Hagen, R. A. Ims, and N. G. Yoccoz. 2008. Climate change and outbreaks of the geometrids *Operophtera brumata* and *Epirrita autumnata* in subarctic birch forest: evidence of a recent outbreak range expansion. Journal of Animal Ecology 77:257–264.

Johnson, D. M., U. Büntgen, D. C. Frank, K. Kausrud, K. J. Haynes, A. M. Liebhold, J. Esper, and N. C. Stenseth. 2010. Climatic warming disrupts recurrent Alpine insect outbreaks. Proceedings of the National Academy of Sciences of the USA 107:20576–20581.

Jones, T., and W. Cresswell. 2010. The phenology mismatch hypothesis: are declines of migrant birds linked to uneven global climate change? Journal of Animal Ecology 79:98–108.

Kerby, J., C. C. Wilmers, and E. Post. 2012. Climate change, phenology and the nature of consumer-resource interactions: advancing the match/mismatch hypothesis. Pages 508–525 *in* T. Ohgushi, O. J. Schmitz, and R. Holt, eds. Trait-mediated indirect interactions: ecological and evolutionary perspectives, Cambridge University Press, Cambridge.

Kudo, G., Y. Nishikawa, T. Kasagi, and S. Kosuge. 2004. Does seed production of spring ephemerals decrease when spring comes early? Ecological Research 19:255–259.

Larsen, E., J. M. Calabrese, M. Rhainds, and W. F. Fagan. 2013. How protandry and protogyny affect female mating failure: a spatial population model. Entomologia Experimentalis et Applicata 146:130–140.

Logan, J. A., J. Régnière, and J. A. Powell. 2003. Assessing the impacts of global warming on forest pest dynamics. Frontiers in Ecology and the Environment 1:130–137.

Lynch, H. J., M. Rhainds, J. M. Calabrese, S. Cantrell, C. Cosner, and W. F. Fagan. 2014. How climate extremes—not means—define a species' geographic range boundary via a demographic tipping point. Ecological Monographs 84:131–149.

McLaughlin, J. F., J. J. Hellmann, C. L. Boggs, and P. R. Ehrlich. 2002. Climate change hastens population extinctions. Proceedings of the National Academy of Sciences of the USA 99:6070–6074.

Memmott, J., P. G. Craze, N. M. Waser, and M. V. Price. 2007. Global warming and the disruption of plant-pollinator interactions. Ecology Letters 10:710–717.

Miller-Rushing, A. J., T. T. Høye, D. W. Inouye, and E. Post. 2010. The effects of phenological mismatches on demography. Philosophical Transactions of the Royal Society B: Biological Sciences 365:3177–3186.

Moran, E. V., S. Bewick, and C. A. Cobbold. 2013. Effects of plant genotype and insect dispersal rate on the population dynamics of a forest pest. Ecology 94:2792–2802.

Morris, W. F. 1997. Disentangling effects of induced plant defenses and food quantity on herbivores by fitting nonlinear models. American Naturalist 150:299–327.

Moscardi, F. 1999. Assessment of the application of baculoviruses for control of Lepidoptera. Annual Review of Entomology 44:257–289.

Murdoch, W. W., B. E. Kendall, R. M. Nisbet, C. J. Briggs, E. McCauley, and R. Bolser. 2002. Single-species models for many-species food webs. Nature 417:541–543.

Parmesan, C. 2006. Ecological and evolutionary responses to recent climate change. Annual Review of Ecology, Evolution, and Systematics 37:637–669.

———. 2007. Influences of species, latitudes and methodologies on estimates of phenological response to global warming. Global Change Biology 13:1860–1872.

Petchey, O. L., U. Brose, and B. C. Rall. 2010. Predicting the effects of temperature on food web connectance. Philosophical Transactions of the Royal Society B: Biological Sciences 365:2081–2091.

Pierle, M. 2010. Beautiful friends, "endangered phenomenon": the life and times of *Danaus plexippus*. Biological Station, University of Michigan (UMBS), Pellston. http://deepblue.lib.umich.edu/bitstream/handle/2027.42/78474/Pierle_Matt_Insects_2010.pdf?sequence=1&isAllowed=y.

Post, E., M. C. Forchhammer, N. C. Stenseth, and T. V. Callaghan. 2001. The timing of life-history events in a changing climate. Proceedings of the Royal Society B: Biological Sciences 2001;268:15–23.

Revilla, T. A., F. Encinas-Viso, and M. Loreau. 2014. (A bit) earlier or later is always better: phenological shifts in consumer-resource interactions. Theoretical Ecology 7:149–162.

Root, T. L., J. T. Price, K. R. Hall, S. H. Schneider, C. Rosenzweig, and J. A. Pounds. 2003. Fingerprints of global warming on wild animals and plants. Nature 421:57–60.

Russell, F. L., and S. Louda. 2004. Phenological synchrony affects interaction strength of an exotic weevil with Platte thistle, a native host plant. Oecologia (Berlin) 139:525–534.

Sherry, R. A., X. Zhou, S. Gu, J. A. Arnone III, D. S. Schimel, P. S. Verburg, L. L. Wallace, and Y. Luo. 2007. Divergence of reproductive phenology under climate warming. Proceedings of the National Academy of Sciences of the USA 104:198–202.

Singer, M. C., and C. Parmesan. 2010. Phenological asynchrony between herbivorous insects and their hosts: signal of climate change or pre-existing adaptive strategy? Philosophical Transactions of the Royal Society B: Biological Sciences 365:3161–3176.

Sparks, T. H., D. B. Roy, and R. L. H. Dennis. 2005. The influence of temperature on migration of Lepidoptera into Britain. Global Change Biology 11:507–514.

Tauber, M. J., and C. A. Tauber. 1976. Insect seasonality: diapause maintenance, termination, and postdiapause development. Annual Review of Entomology 21:81–107.

Thackeray, S. J., T. H. Sparks, M. Frederiksen, S. Burthe, P. J. Bacon, J. R. Bell, M. S. Botham, et al. 2010. Trophic level asynchrony in rates of phenological change for marine, freshwater and terrestrial environments. Global Change Biology 16:3304–3313.

Tobin, P. C., S. Nagarkatti, G. Loeb, and M. C. Saunders. 2008. Historical and projected interactions between climate change and insect voltinism in a multivoltine species. Global Change Biology 14:951–957.

Umbanhowar, J., and A. Hastings. 2002. The impact of resource limitation and the phenology of parasitoid attack on the duration of insect herbivore outbreaks. Theoretical Population Biology 62:259–269.

van Asch, M., and M. E. Visser. 2007. Phenology of forest caterpillars and their host trees: the importance of synchrony. Annual Review of Entomology 52:37–55.

Vasseur, D. A., and K. S. McCann. 2005. A mechanistic approach for modeling temperature-dependent consumer-resource dynamics. American Naturalist 166:184–198.

Visser, M. E., and C. Both. 2005. Shifts in phenology due to global climate change: the need for a yardstick. Proceedings of the Royal Society B: Biological Sciences 272:2561–2569.

Visser, M. E., and L. J. M. Holleman. 2001. Warmer springs disrupt the synchrony of oak and winter moth phenology. Proceedings of the Royal Society B: Biological Sciences 268:289–294.

Watt, A. D., and A. M. McFarlane. 2002. Will climate change have a different impact on different trophic levels? phenological development of winter moth *Operophtera brumata* and its host plants. Ecological Entomology 27:254–256.

White, R. R. 1974. Food plant defoliation and larval starvation of *Euphydryas editha*. Oecologia (Berlin) 14:307–315.

Zalucki, M., and Y. Suzuki. 1987. Milkweed patch quality, adult population structure, and egg laying in the monarch butterfly. Journal of the Lepidopterists' Society 41:13–22.

Zhang, X., D. Tarpley, and J. T. Sullivan. 2007. Diverse responses of vegetation phenology to a warming climate. Geophysical Research Letters 34:L19405. doi:10.1029/2007GL031447.

Zonneveld, C. 1992. Polyandry and protandry in butterflies. Bulletin of Mathematical Biology 54:957–976.

Zonneveld, C., and J. A. J. Metz. 1991. Models on butterfly protandry: virgin females are at risk to die. Theoretical Population Biology 40:308–321.